Synthetic hydrogels: 3. Hydroxyalkyl acrylate and methacrylate copolymers: surface and mechanical properties

Andrew Barnes, Philip H. Corkhill and Brian J. Tighe*

Speciality Materials Research Group, Department of Chemical Engineering and Applied Chemistry, Aston University, Aston Triangle, Birmingham B4 7ET, UK

(Received 3 February 1988; revised 19 April 1988; accepted 16 May 1988)

The surface and mechanical properties of copolymers of hydroxyalkyl acrylates and methacrylates have been examined by a variety of techniques. This work is complementary to earlier parts of this series which describe the effect of copolymer structure on water binding properties. Water structure has been demonstrated to exert a profound effect upon mechanical properties whether measured in compression or in tension. In particular, water that is characterized by differential scanning calorimetry as 'freezing' water is observed to have a marked plasticizing effect upon the gel, whereas 'non-freezing' water has little such effect. Similarly, the 'freezing' water produces a more marked effect on thermally induced transitions. Two distinct transition points are observed as a result of its presence. One corresponds to the freezing point of water and the other to a glass transition temperature, whose value depends upon the proportion of 'freezing' or 'plasticizing' water in the gel. Several predictive and direct measurement techniques have been used to study the surface properties of the copolymers in both hydrated and dehydrated states. Taken together they have established a sound understanding of the way in which polar and dispersive components of surface free energy vary as a function of copolymer composition and water content. Use of protein adsorption and fibroblast cell interaction techniques demonstrate that biological phenomena respond to changes at a molecular level which current macroscopic surface energy techniques are unable to discern.

(Keywords: hydrogel; protein adsorption; hydroxyalkyl acrylates; hydroxyalkyl methacrylates; surface properties; mechanical properties)

INTRODUCTION

In a preceding part of this series we have described the effect of copolymerization with relatively hydrophobic monomers on the equilibrium water content (*EWC*) and water binding properties of the hydroxyalkyl acrylates and methacrylates[1]. The resultant changes, both in total water content and in the fraction of 'freezing water' within the gel, exert a marked effect on the related surface and mechanical properties of these materials. Despite the fact that water structuring plays an important part in controlling the permeation properties of the hydrogel, the usefulness of this fact is, in many cases, compromised by undesirable changes in mechanical strength. Techniques for measurement of surface and mechanical properties of hydrogels in a reproducible and unambiguous manner are difficult to establish. This is in part due to the inherent properties of the materials but to a large extent is related to the difficulties associated with the loss of water from the gel, when held in a non-aqueous environment. We present here some useful techniques and novel approaches related to these problems and, in particular, their application to copolymers of the hydroxyalkyl acrylates and methacrylates with relatively hydrophobic monomers.

EXPERIMENTAL

Monomers

Optical-grade 2-hydroxyethyl methacrylate was supplied by Ubichem Ltd with a certificate of analysis. Hydroxypropyl acrylate (BDH), hydroxyethyl acrylate (BDH), hydroxypropyl methacrylate (BDH), styrene (BDH), ethyl methacrylate (BDH), methacrylic acid (Koch Light) and methyl methacrylate (BDH) monomers were purified by reduced-pressure distillation[1]. Ethyleneglycol dimethacrylate (BDH) and azobisisobutyronitrile (Aldrich) were used as supplied.

Preparation of membranes

Xerogels were prepared by copolymerizing the monomers *in situ* between two glass plates separated by a gasket, as previously described[1].

Equilibrium water content

The *EWC* was calculated by weight difference as described in the first paper of this series[1]. Small samples were cut from a hydrated sheet of the hydrogel and, after the surface water had been removed, the samples were weighed then dehydrated overnight in a vacuum oven to constant weight. The *EWC* (100% × weight of water in the gel/total weight of hydrated gel) was calculated and the final value is an average of at least three determinations.

Surface properties

The surface energies of the hydrogels were probed using Hamilton's method, captive air bubble and conventional sessile drop techniques.

Hamilton's method[2]. Surface water was wiped from one side of the sample, which was glued to a glass cover slip. The sample was then suspended inverted in an optical cell,

* To whom correspondence should be addressed

0032-3861/88/122191-12$03.00

which was then filled with distilled water saturated with n-octane. A small drop of n-octane was placed on the sample surface through a G25 syringe needle, whose point had been removed by grinding in order that the drop was formed symmetrically on the sample surface.

Angular measurements were taken for both the left and right contacting drop interfaces and then averaged. This was repeated for at least three different octane droplets and the overall average value was taken. Contact angle measurements were either made directly, using a travelling telescope with a goniometer eyepiece equipped with a crosswire and angular scale, or by the photographic technique described below (sessile drop technique). Hamilton showed that as both n-octane and water have the same dispersive component of their surface free energies, 21.8 mN m^{-1}, the dispersive component of the surface free energy of the sample cancels out, which means that the polar component of the sample may be evaluated directly.

Captive air bubble technique. For this technique the sample is mounted underwater in exactly the same way as for the Hamilton method. Instead of an n-octane droplet, however, an air bubble is released onto the sample surface. A specially curved G35 needle (2.032×10^{-4} m diameter) was obtained from Aston Needles Inc. for this work. Use of this needle in conjunction with a 'Prior' micromanipulator enabled an air bubble to be delivered onto the sample surface, from a microsyringe, in such a way that the needle can be inserted into the air bubble so that its volume can be precisely controlled. The air bubble was enlarged to a diameter of approximately 5–6 mm and then reduced down to a size of 2 mm and the needle retracted. The contact angle measurements were then taken in a similar manner to that used in the Hamilton method and an average value taken.

Sessile drop technique. Prior to contact angle measurement the polymer surfaces were cleaned by washing with a detergent solution and then rinsing thoroughly in distilled water before drying the samples in a vacuum desiccator. The sessile drop of the wetting liquid was formed on the surface of the polymer through a G25 hypodermic needle, the position of which could be accurately controlled with the aid of a Prior micromanipulator. By supporting the polymer sample in a glass cell with optically perfect sides the enclosing atmosphere could be controlled and the sample isolated from air currents. Use of a Rank Aldis Tutor 2 projector fitted with a short, 5 cm, focal length lens enabled an enlarged image of the sessile drop to be projected onto a back-projection screen. A photograph of the image was then taken for later examination. The contact angle was measured by drawing a tangent to the drop surface at the three-phase interface and measuring the angle with a protractor. At least six measurements were made on each polymer sample and each measurement was the average of the contact angles on either side of the sessile drop. Averaged values lay within a $\pm 2°$ band. Standard samples of polymer surfaces were regularly used as internal checks on the reproducibility of the procedures.

This technique may be used in conjunction with the Owens and Wendt equation (equation (1))[3] to determine the surface free energies of polymers in the dehydrated state:

$$1+\cos\theta=(2/\gamma_{lv})[(\gamma_{lv}^{d}\gamma_{s}^{d})^{0.5}+(\gamma_{lv}^{p}\gamma_{s}^{p})^{0.5}] \quad (1)$$

where θ is the contact angle of the wetting liquid with the solid, γ_{lv} the liquid–vapour interfacial free energy, γ_s the solid surface free energy and the superscripts p and d refer to the polar and dispersive fractions of the surface or interfacial free energy.

Two wetting liquids which have been fully characterized for polar and dispersive components are used. By measuring the contact angles of the liquids on the polymer surface and solving the equations simultaneously, γ_s^p and γ_s^d, the polar and dispersive components of the surface free energy of the polymer, may be determined.

Surface properties: predictive methods

One of the important aspects of polymer science is the correlation of the structure of polymers with their chemical and physical properties. Direct measurement may be difficult and in these cases predictive techniques provide a useful basis for comparison. Two predictive techniques, the parachor and cohesive energy density, were used in this work to predict surface energies and the predicted values were compared with experimental values.

Parachor. In 1923 Macleod[4] discovered a simple relationship connecting the surface tension or free energy of a liquid and its density:

$$\gamma=C(D-d)^4 \quad (2)$$

where D and d are the densities of the liquid and its vapour, γ is the surface tension at the same temperature and C is a constant characteristic of the liquid. Fowler[5] has shown that this expression may be deduced theoretically.

Sugden[6] revised the Macleod equation to express the constant in molar proportions and called this new constant the parachor P:

$$P=\frac{M\gamma^{1/4}}{(D-d)} \quad (3)$$

where M is the molecular weight and P is the parachor. When the vapour density is small in comparison with that of the liquid, the expression reduces to:

$$\gamma=\left(\frac{PD}{M}\right)^4 \quad (4)$$

i.e.

$$\gamma=\left(\frac{P}{V_m}\right)^4 \quad (5)$$

where V_m is the molar volume of the liquid.

The parachor was first thought to be an additive function but further examination of previous work[7,8] showed that certain constitutive features such as double bonds, rings and chain branching can be assigned values. Calculations of γ were carried out using the parachor values of Quayle[9].

Cohesive energy density. Hildebrand and Scott[10] applied an empirical but accurate relationship to connect surface tension, cohesive energy density and molar volume for non-polar liquids. This was modified by Wu[11] to provide

accurate predictions for polymers based on molecular constitution. The relationship can be stated as:

$$\gamma = 0.327\left(\frac{(\Sigma F)_s}{n_s}\right)^{1.85}\left(\frac{n_s}{v_s}\right)^{1.52} \quad (6)$$

where n_s is the number of atoms in the segment, $(\Sigma F)_s$ is the summation of Small's[12] force constants for the segments and v_s is the molar volume of the repeat unit. In developing this equation Wu presumes that Small's values of F give the dispersion force contribution to surface tension and that the value of γ given by this equation is equal to the dispersion part of the total surface free energy.

Protein adsorption

For protein adsorption studies the following reagents were used: human serum albumin (fraction V; 96–99% pure, remainder mainly globulins, Sigma), human fibrinogen (fraction 1; >90% of protein clottable, Sigma), iodinated [^{125}I] human albumin injection (specific activity = 2.5 mCi/mg albumin, Amersham International), iodinated [^{125}I] human fibrinogen injection (specific activity > 100 mCi/mg fibrinogen, Amersham International) and tris(hydroxymethyl)aminoethane (Sigma). All protein solutions were made up in physiological Krebs solution (pH 7.4).

Both static and dynamic measurements of protein adsorption with time were made for each hydrogel under investigation. Using dynamic adsorption studies, only five hydrogel samples could be examined at one time and the system was wasteful, using large amounts of radiolabelled protein solution. To overcome these problems a static adsorption technique was developed which enabled a statistically significant number of samples, of a large number of copolymers, to be examined over a series of 12 time intervals. This technique gave results that were consistent with the dynamic method. The apparatus used in these studies was of relatively simple design and construction, enabling multiple simultaneous analyses. A gentle 'rocking' agitation of a sealed vial (which contained the sample) was employed to maintain steady movement of the solutions over the polymer interface. All adsorption studies were carried out at 20°C, unless the effect of temperature was being studied.

The samples were placed in 20 ml vials and 2 ml of Krebs solution, followed by 2 ml of radiolabelled protein solution, were added to each sample. The times were noted and at this point 3 × 100 ml aliquots were taken from the radiolabelled protein 'stock' solution to be used as internal counting standards. The vials were sealed and stored in the dark until the prescribed time had elapsed, whereupon the radiolabelled solution in each vial was displaced from the samples by a volume displacement method using 500 ml of Krebs solution, at room temperature, and at a flow rate of 100 ml min^{-1}. It had been established that this flow rate was effective in eliminating all the radiolabelled solutions from the vials, leaving the samples suspended in Krebs solution. The efficiency of the 'washing' procedure was monitored by taking 1 ml aliquots of this latter suspending Krebs solution. The samples were then carefully transferred to counting vials and sealed in preparation for γ counting.

All samples ready for counting were loaded into the γ counter (Nuclear Enterprises type 8312) together with the internal standards and a requisite number of blanks for both the estimation of background radiation and to act as experimental controls. Machine counting efficiency was determined for the ^{125}I isotope by the conventional procedures from which the optimum operating conditions were obtained. Each sample was counted for 2×10^5 counts or 600 s (whichever elapsed first). As ^{125}I has a half-life of 60 days, for the typical total counting time of 6 h for 60 samples, the decay during this period is insignificant. The mean adsorbed protein was then calculated using internal standards, after correcting for background radiation.

Mechanical properties

Microindentation studies. The deformation properties of the hydrogels were studied using a modified form of the R.E.L. pneumatic microindentation hardness apparatus, originally developed to correlate the deformation properties of surface coatings with their ageing properties[13,14]. The measurement of the deformation of the test sample under a load is carried out by a pneumatic method. The principle is that the displacement of the indentor needle, due to deformation of the test sample under a load, alters the gap between a flapper and a small nozzle fed with a restricted gas supply. The resulting gas pressure is amplified and applied to a pneumatic recorder. A schematic diagram of the apparatus is shown in *Figure 1* and the principles of its operation are described below.

Nitrogen at 20 psi enters the system at A and is divided into three streams. One stream of the nitrogen gas is carried, via a flow restrictor, into a programmer and then out again to the weight lowering bellows B_1 via another flow restrictor. The second stream of nitrogen is led to the nozzle N_1 and the proximity of the flapper to the nozzle N_1 determines the pressure developed in the bellows B_2. This operates the flapper F_2 of a single-stage amplifier with feedback. The third stream of nitrogen gas is led to another nozzle N_2, and the proximity of the flapper F_2 to the nozzle N_2 determines the pressure in the bellows B_3 and at the recorder. Expansion of the bellows B_3, by increasing pressure, bends the beam J and tends to increase the separation of F_2 and N_2. This applies a negative feedback to the second stage which reduces the gain, but improves the linearity and stability of the output. The results were recorded on a 0–15 psi strip chart nitrogen pressure recorder (Akron model 63).

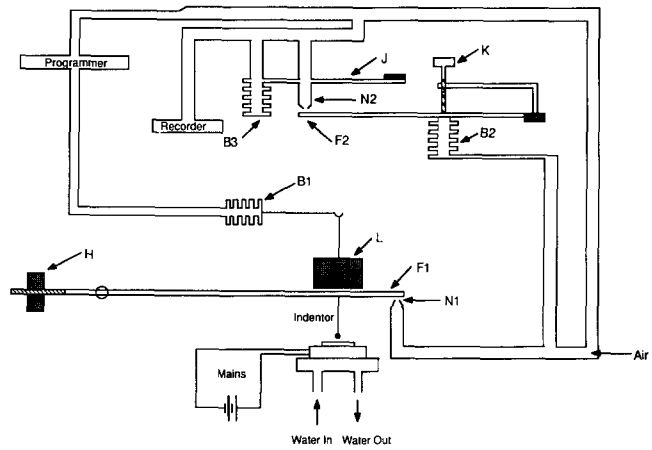

Figure 1 A schematic diagram of the apparatus used for micropenetrometry studies (see text for details and key)

An 8×10^{-3} m diameter spherical indentor was used for this work together with various weights in the range 0.14–16 g. The recorder was calibrated to give a full-scale deflection in the range 6–30 μm, depending on the modulus of the material under test. The sample stage of the instrument was equipped with an electrically controlled unit which enabled the temperature to be varied between -50 and $+90$°C. In addition, water circulation through the cored stage is provided as a means of temperature stabilization. All the work described in this paper was carried out at 20°C.

The samples under test were prepared as follows: All dehydrated samples were glued to microscope slides with an α-cyanoacrylate adhesive and left overnight before further use. For deformation measurements on hydrated samples, a sample of measured thickness was placed on a microscope slide ensuring a good contact; the surface of the hydrogel was then covered with a thin layer of paraffin oil to prevent evaporation of water during the deformation measurements. The microscope slide supporting the sample was placed on the specimen stage and secured. The beam was then lowered until the indentor needle touched the test sample and the chart recorder adjusted to read zero. A test weight was placed in position and pneumatically lowered onto the beam when the programmer was activated. The indentation and recovery curves were recorded automatically, the timescale being normally set to 1 min for both indentation and recovery. A second indentation and recovery curve was recorded on the same part of the test specimen. This procedure was repeated at three or four different points on the test specimen for a single load. The load on the indentor was then increased and the deformation experiments were repeated for several loads on the same sample. A series of standard materials ranging from elastomers to thermoplastics were regularly used to check the operation of the system and reproducibility of the determinations. Although the reproducibility of the measurements is no greater than $\pm 10\%$, these results are quite acceptable given that the moduli of the samples vary over three orders of magnitude. The Young's and rigidity moduli were calculated using the equations of Hertz[15] (equation (7)) and Taylor and Kragh[16] (equation (8)):

$$\frac{E}{1-\nu^2} = \frac{3}{4}\frac{mg}{r^{0.5}h^{1.5}} \tag{7}$$

$$G = 0.36\frac{mg}{r^{0.5}}\left(\frac{t-h}{h}\right)^{1.5} \tag{8}$$

where E is Young's modulus, G the rigidity modulus, ν the Poisson ratio of the material, m the load, g the acceleration due to gravity, r the radius of the indentor, h the depth of indentation and t the thickness of the sample.

Tensile properties. The tensile properties of the hydrogels were investigated using a Testometric Micro 500 tensometer (with 100 N load cell), interfaced with an Apple IIe computer and an Iiwatso SR6602 plotter. Samples of 6.25 mm width were cut from the hydrogel under test and these were held between the rubberized jaws of the tensometer. The tests were carried out using a crosshead speed of 10 mm min^{-1} and a gauge length of 10 mm. The tensile strength, elongation to break and Young's modulus of the sample under test were calculated. In addition, the program enabled stress–strain and load–elongation curves to be plotted and performed a statistical analysis of the five tests run on each sample.

RESULTS AND DISCUSSION

Surface properties: dehydrated polymers

Our initial interest in determining the detailed surface energies of dehydrated hydroxyalkyl acrylate copolymers arose from our work on melt-processable, substantially linear, versions of these materials. The problems associated with direct measurements on the molten polymers stimulated an interest in the predictive techniques, based on calculations using the parachor and cohesive energy density. The history of these techniques in relation to the melt properties of conventional polymers is well known and in many cases good correlaton between experimentally determined and calculated values are obtained[17]. The application of results obtained in this way to the melt processability of the hydroxyalkyl acrylates is described elsewhere[18]. The predictive techniques provide a useful basis for the consideration of the surface properties of the resultant hydrated hydrogels, in addition to the interest which they generate in their own right. *Table 1* presents the appropriate parameters for use in the cohesive energy density-based (equation (6)) and parachor-based (equation (5)) calculations of the surface energies of the copolymers described here. The resultant calculated surface energies are contained in *Table 2* together with the experimentally determined polar and dispersive components, measured by the technique of Owens and Wendt[3]. The first point of interest, arising from these observations, is that the total surface energies of the hydroxyalkyl acrylates and methacrylates are not dissimilar to those of conventional vinyl and acrylic copolymers, such as polystyrene and poly(methyl methacrylate). A marked difference does arise, however, when the separate contributions of polar and dispersive components are taken into account, since these are markedly different in the two groups of materials. Thus, in the case

Table 1 Parameters used for the cohesive energy density-based and parachor-based predictions of surface energy

Monomer	Molecular weight (g mol^{-1})	Density (gm cm^{-3})	Parachor	ΣF	No. of atoms in repeat unit, n_s
Hydroxyethyl methacrylate	130	1.28	270.7	1000	19
Hydroxypropyl methacrylate	144	1.24	310.7	1109	22
Hydroxyethyl acrylate	116	1.36	234.4	907	16
Hydroxypropyl acrylate	130	1.24	274.4	1016	19
Methyl methacrylate	100	1.19	216.4	778	15
Styrene	104	1.07	245.4	896	16
N-vinylpyrrolidone	111	1.21	245.3	910	17

Table 2 Comparison of calculated and predicted surface energies of dehydrated hydroxyalkyl acrylate and methacrylate copolymers

Composition	CED-predicted γ^d	Surface energy calculated from Owens and Wendt equation			Parachor-predicted γ^t
		γ^d	γ^p	γ^t	
HEMA–St					
100/0	39.1	31.4	20.2	51.6	50.5
90/10	38.7	31.7	18.8	50.5	49.2
50/50	37.5	32.1	14.9	47.0	45.0
30/70	36.9	32.8	12.3	45.1	43.2
10/90	36.5	35.3	7.3	42.6	41.4
0/100	36.1	40.2	1.9	42.1	40.6
HEA–St					
100/0	45.1	37.4	19.1	56.5	57.0
90/10	44.2	36.2	19.7	55.9	56.1
80/20	43.3	35.3	20.1	55.4	54.1
50/50	40.7	33.3	19.9	53.2	49.3
40/60	39.8	31.9	20.0	51.9	47.6
30/70	38.9	30.9	20.5	51.4	45.9
10/90	37.1	29.6	19.9	49.5	42.5
0/100	36.1	40.2	1.9	42.1	40.6
HPMA–St					
100/0	39.5	33.1	16.6	49.7	43.5
50/50	37.7	34.7	13.8	48.5	41.2
0/100	36.1	40.2	1.9	42.1	40.6
HPA–St					
100/0	34.9	31.8	19.0	50.8	51.2
70/30	35.1	35.2	15.3	50.5	47.3
50/50	35.3	31.2	19.1	50.3	45.0
30/70	35.6	34.2	14.0	48.2	43.0
20/80	35.7	30.5	15.7	46.2	41.3
10/90	35.9	30.5	15.7	46.2	40.6
0/100	36.1	40.2	1.9	42.1	40.6
HEMA–MMA					
100/0	39.1	31.4	20.2	51.6	50.5
75/25	38.2	36.7	12.7	49.4	48.5
50/50	37.3	41.3	7.9	49.2	46.8
25/75	36.3	39.5	6.9	46.9	45.3
0/100	35.4	35.4	5.4	46.9	44.0

of dehydrated poly(2-hydroxethyl methacrylate), poly-(HEMA), for example, the polar fraction of the total surface energy is around 0.4, whereas in the case of poly(methyl methacrylate) it is less than 0.2. Furthermore, it is evident in all cases that incorporation of relatively small amounts of polar monomer appears to have a disproportionately large effect on the measured, as distinct from calculated, surface energies of copolymers. It is further evident that the hydroxyalkyl methacrylates give better agreement between predicted and measured values than their counterpart acrylates.

Surface properties: hydrated polymers

The importance of the polar component of surface free energy becomes even more marked in the hydrated gels. This is shown in *Figure 2* which illustrates that, in this series of materials, the polar fraction arises from a vanishingly small value in polystyrene to the point where it dominates the surface energy in poly(HEMA) hydrogel. Taking the dehydrated values as a baseline, this reflects the inevitable consequence of incorporating increasing quantities of a liquid (water) having a polar component of 51 mN m^{-1} and dispersive component of 21.8 mN m^{-1}. It illustrates the particular interest in these families of hydrogels in which the transition from a dispersive-dominated to a polar-dominated surface occurs. The values shown have been obtained by a combination of techniques. Curves A and B show the polar and dispersive components derived from a combination of the measured values for the dehydrated polymer (*Table 2*) and the known values for bulk water. The components of the hydrated gel are then calculated on the basis of the volume fraction of water and of polymer present at each composition. No distinction has been made between different water binding states, but a similar calculation predicts the difference in surface energies between alkyl methacrylates and hydroxyalkyl methacrylates to within 5% of the measured values. The polar components of the styrene–HEMA based hydrogels measured directly by the Hamilton technique are shown in curve C. *Figure 3* presents further information as a function of changing water content in the gel. These results, which are based on copolymers of a wide range of hydroxyalkyl acrylates and methacrylates, show the measured polar component (Hamilton technique, curve A) together with the measured dispersive component (curve B). This latter value has been obtained by insertion of the measured polar components, together with the measured water/air contact

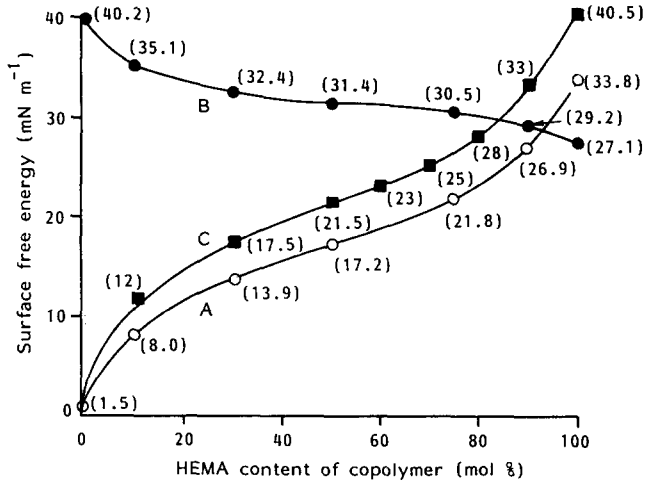

Figure 2 Calculated polar (A) and dispersive (B) components of the surface free energy of hydrated styrene–HEMA based hydrogels. Values of the polar component (C) measured by the Hamilton technique are shown for comparison

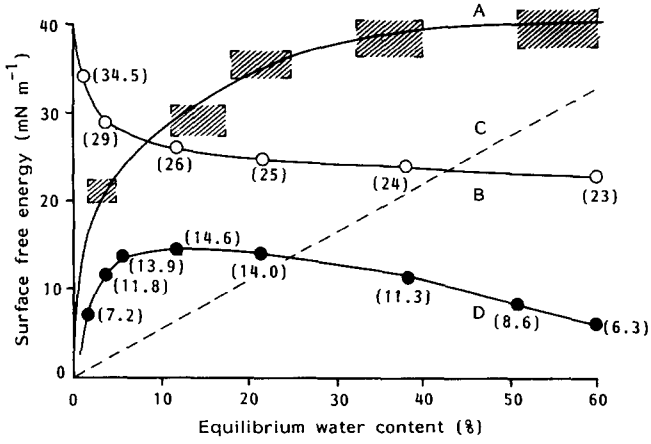

Figure 3 Measured polar (A) and dispersive (B) components of the surface free energy of hydroxyalkyl acrylate and methacrylate copolymers shown as a function of *EWC*. The separate calculated contributions of water (C) and polymer (D) to the polar component are also shown

angles, into the Owens and Wendt equation. Because of the uncertainties inherent in the Hamilton method, curve A illustrates the spread of measurements, made by several workers on some 50 gels, in these laboratories.

Several problems that are not encountered in determining values for non-water-containing polymers exist in the measurement of surface properties of hydrogels. These problems are associated with the fact that water plays an integral part in the establishment of the surface properties of the system and yet it is its very presence that makes direct droplet measurements at the surface difficult. The use of water immersion (captive air bubble and octane droplet) techniques maintains the surface in a hydrated state but makes it difficult for the droplet probes to displace the adsorbed water layers. For this reason the results are modified by this water layer. In other studies on adsorbed species on polymer surfaces we have demonstrated that the values of the surface energy components of such systems are a function of both adsorbed and substrate layers[19]. The difference between the derived (*Figure 2*, curve A) and directly measured (*Figure 2* curve C) polar components of the styrene– HEMA based hydrogels may reflect a similar phenomenon. Additionally, interfacial contact angles produced at such hydrophilic surfaces are difficult to measure accurately and reproducibly.

Conventional sessile drop in air techniques, on the other hand, present different but related problems. The use of measurements involving water droplets on freshly blotted gel surfaces suffer from the disadvantage that the surface layer dehydrates rapidly and becomes relatively hydrophobic. If a residual aqueous film is left intact before the water droplet is applied the surface is unrepresentatively hydrophilic. The essence of the problem lies in the fact that the interface between a hydrogel surface and water is much more diffuse than that between conventional hydrophobic polymers and water. The differences between the two methods of determining the polar components shown in *Figure 2* (curves A and C) reflect this fact. Some studies have been carried out by Andrade and his group on copolymers of HEMA with methoxyethyl methacrylate using air bubble and octane droplet techniques[20]. Our work with styrene copolymers and using other hydroxyalkyl acrylates and methacrylates produces the same trends, although with small but significant differences in detailed values.

It is instructive to calculate the interfacial tension (γ_{WH}) between water (W) and the hydrogel (H) surface using, for example, the geometric mean technique:

$$\gamma_{WH} = \gamma_W + \gamma_H - 2(\gamma_W^p \gamma_H^p)^{0.5} - 2(\gamma_W^d \gamma_H^d)^{0.5} \qquad (9)$$

The superscripts p and d once again refer to the polar and dispersive components of interfacial free energy. A direct correlation can be made with the magnitude of the water sessile drop contact angle obtained in air on a hydrogel surface from which excess water has been previously removed. There is general agreement that this value is around 20° for poly(HEMA) hydrogel and will rise with HEMA–styrene copolymers to a value of around 90° for polystyrene. Values for the interfacial tensions between water and the hydrogels derived from this copolymer series and water are most conveniently derived from equation (9) in conjunction with the information contained in *Figure 2*. Andrade's results suggest that virtually no measurable changes occur in gels containing more than 20% water by weight and that the interfacial tension is already zero at this point. Our results indicate a continuous variation between 20% and 60% *EWC*, a trend continued in a series of hydrogels having higher water contents[21]. The interfacial tension falls from around 1.6 mN m^{-1} at 20% *EWC* to around 0.8 mN m^{-1} at 60% *EWC*. These small but real values of interfacial tension accord with the fact that the water contact angle does not fall to zero within this range of polymers. We find, significantly, that the polymer structure is capable of influencing the detailed surface energy components throughout this range. The calculated relative contributions of polymer and water to the polar component of the surface energy, as a function of fractional hydration, is shown in *Figure 3* (curves C and D). The use of measurements on dehydrated surfaces in this manner illustrates the way in which the surface energy parameters of hydrogels should be affected by polymer structure. They support the view that the direct measurement techniques currently available for hydrated surfaces produce the impression of a surface layer of water that dominates the measured values. Molecular processes at hydrogel surfaces (e.g. biological interaction and protein deposition) indicate that surface changes, inadequately detected by macroscopic droplet techniques, take place as the nature of the polymer matrix and the volume fraction of water are varied. Calculations of the type shown in *Figure 3* (curves C and D) reflect such changes.

The interfacial tension obviously plays an important part in governing bio-interactions at hydrogel surfaces. This is a complex area because biological fluids contain naturally occurring wetting agents whose size generally precludes them from entering the hydrogel matrix. Their surface tensions (typically around 50 mN m^{-1}) are thus lower than that of water and, initially, lower than that of the water-swollen matrix. This situation is modified by subsequent biological deposition at the polymer surface. In the case of hydrogels for biomedical applications, therefore, a low interfacial tension with water is not necessarily a relevant guide to compatibility. In considering membrane transport through aqueous media, however, the interfacial tension is of more direct predictive use. It is well known that transport from aqueous media across hydrophobic membranes induces the so-called barrier effect at the interface[22,23]. Thus, the predicted increase in flux with decreasing membrane thickness is offset by the greater proportional importance of the barrier effect as the thickness of the membrane is reduced. As the hydrophilicity or water content of the membrane is increased, and the interfacial tension with water correspondingly reduced, the contribution of the barrier effect diminishes.

Surface properties: protein adsorption

The difference between surface properties sensed by droplet techniques and those sensed at molecular level by proteins is quite marked. Although protein adsorption studies are conventionally carried out in an attempt to correlate the thrombogenic behaviour of different materials, that is not the purpose here. The different affinities of albumin and fibrinogen for molecular sites in materials has been a matter of considerable debate. Their use here is designed simply to illustrate the existence of structural changes that are capable of dominating molecular events at hydrated surfaces. Preliminary studies

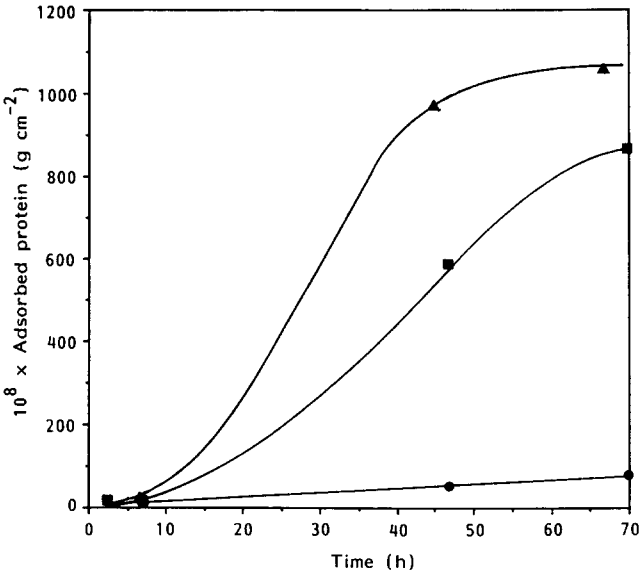

Figure 4 Effect of temperature on the fibrinogen adsorption profile for poly(HEMA) hydrogels at (▲) 37°C, (■) 20°C and (●) 4°C

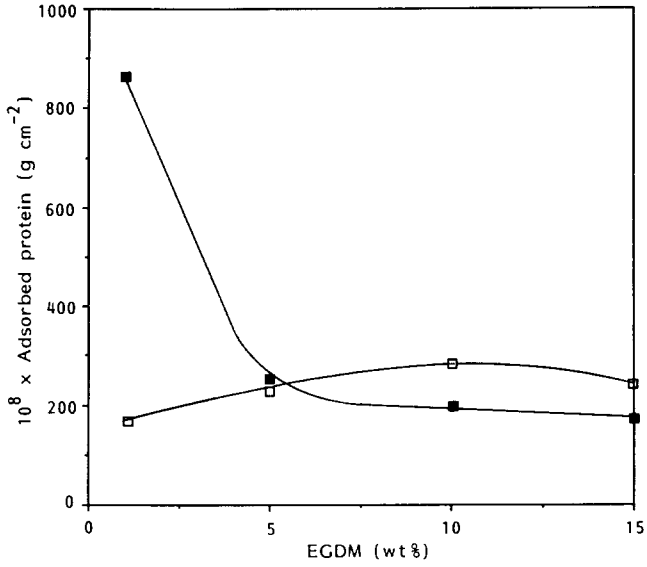

Figure 5 Effect of ethyleneglycol dimethacrylate content on the adsorption of (■) fibrinogen and (□) albumin onto crosslinked poly(HEMA) hydrogels

readily reflect this and underline the importance of monomer purification and reproducibility of preparation in such work. Thus, hydrogels based on HEMA purified in different ways and consequently containing different levels of methacrylic acid impurity show apparent differences in fibrinogen adsorption. This illustrates the importance of analytical techniques in conjunction with preparation procedures in order to produce well characterized monomers.

Careful control of experimental conditions in protein adsorption studies is also necessary and the regular use of standard surfaces to ensure the reproducibility of results is essential. Although adsorption levels are measured as a function of time (*Figure 4* illustrates the influence of time and temperature in this respect) results presented here are those taken after 70 h. *Figures 5* and *6* illustrate the effect on fibrinogen and albumin adsorption of reducing water content by incorporation of ethyleneglycol dimethacrylate (EGDM, *Figure 5*) and styrene (*Figure 6*). The effect of EGDM incorporation on water content has been described in detail in a previous paper[1]. It is apparent that small amounts of crosslinking agent cause a dramatic drop in fibrinogen adsorption to a plateau value whilst albumin adsorption remains virtually unaffected, showing results that might be interpreted as an initial steady rise followed by a slight fall with increasing EGDM incorporation. A parallel effect is observed with styrene (St) incorporation. Thus, a decrease in fibrinogen adsorption to a plateau value is observed together with an initial rise in albumin adsorption followed by a subsequent decline.

It might be reasonable to suggest that these figures reflect two regimes of behaviour. There is a general tendency for albumin and fibrinogen adsorption to move in opposite directions, which occurs in the compositional range where the copolymers could be described as gels. In this region *EWC* values lie between 25 and 40% corresponding to styrene contents of 10% or less. As the comonomer contents rise to around 20%, however, and water plays a much less dominant role in the materials, albumin and fibrinogen adsorption fall together. *Figure 7* appears to support this view; here the HEMA copolymer with ethyl methacrylate (EMA) may be compared to the styrene copolymer in *Figure 6*. The same trend is shown, but at higher EMA comonomer values relative to those observed with styrene. This might be taken to reflect the less efficient reduction in water content that EMA induces. A further point of interest in *Figure 7* is the behaviour observed with vinylpyrrolidone (VP) incorporation. Here the water content rises as the comonomer increases (the 50/50 HEMA–VP copolymer has an *EWC* of 64%). Fibrinogen adsorption is observed to rise with this increase in water content and although this does appear to fit the trend of adsorption and water content presented here, it must be remarked that VP copolymers were observed to show fibrinogen adsorption strikingly different from any other of the various families of hydrogels studied[21]. In contrast, the steady rise in

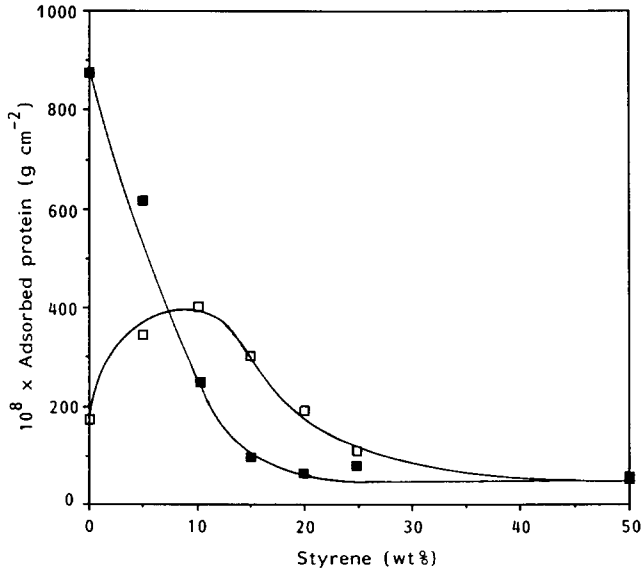

Figure 6 Effect of styrene incorporation on the adsorption of (■) fibrinogen and (□) albumin onto HEMA–St copolymer hydrogels

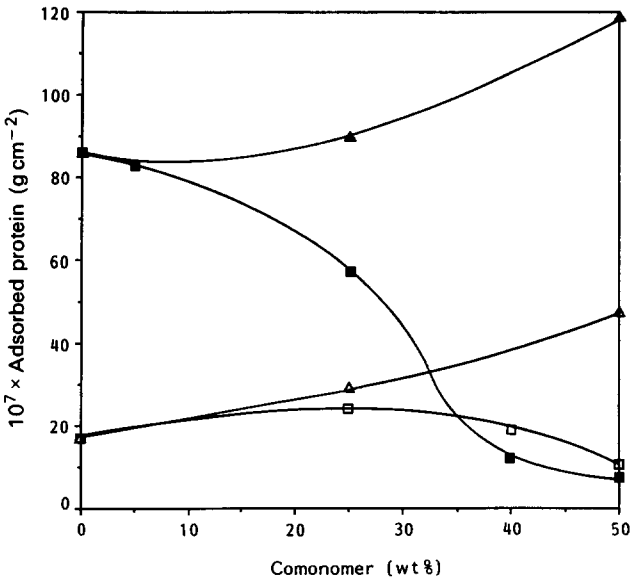

Figure 7 Effect of ethyl methacrylate incorporation on (■) fibrinogen and (□) albumin adsorption on HEMA–EMA copolymer hydrogels, contrasted with the effect of *N*-vinylpyrrolidone incorporation on the adsorption of (▲) fibrinogen and (△) albumin on HEMA–VP copolymer hydrogels

albumin adsorption with increasing water content of the VP–HEMA copolymers also shown in *Figure 7* is quite characteristic of the behaviour shown with high-water-content hydrogels. The changes reflected in *Figures 5–7* correspond to relatively narrow water content range of neutral hydrogels. They illustrate the marked changes that occur in protein adsorption when relatively small changes in surface chemistry are made. They are not intended to reflect the broad trends in albumin and fibrinogen adsorption that occur on surfaces of more widely varying hydrophilicity[21].

The effect of surface charge is important and the results shown in *Figure 8*, in which methacrylic acid (MAA) is progressively incorporated in a series of HEMA copolymers, reflects those observed in acrylamide–MAA systems[21]. The incorporation of relatively small amounts of carboxyl groups (which exist as the carboxylate anion in physiological solutions) produces a dramatic reduction in both fibrinogen and albumin adsorption. Although these various trends may reasonably be correlated with the effect of charge and hydration, it is evident that the changes in adsorption behaviour are much more marked than the measured changes in surface properties of which current techniques are capable. This fact is undoubtedly a reflection of the differences between surface probes which operate on the macroscopic and on the molecular level. Dramatic differences are also observed in the interaction of animal (fibroblast) cells with hydrogel surfaces of the type described here. This, in turn, is a function of the interfacial conversion processes that occur when hydrogels are placed in contact with biological systems and again reflects behaviour at a molecular level[24–26].

Mechanical properties

The mechanical properties of hydrogel polymers are not easy to measure. The very act of deformation involved in such testing procedures produces redistribution of the water in the specimen and the properties determined for hydrated polymers rarely reflect those of the material determined in the normal fashion. Nonetheless, such measurements are made and give useful comparative information. We have, in previous work, constructed test cells which enabled tensile testing to be carried out with complete immersion in the appropriate aqueous medium. Perhaps surprisingly, the form of the tensile stress–strain curves produced did not show appreciable differences from measurements made in air, provided sufficient speed and care were taken to prevent premature dehydration of the sample. *Figure 9* shows tensile load–extension curves for poly(HEMA) and for three HEMA–MMA copolymers in which the effect of increasing hydrophobic monomer content and concurrent decrease in *EWC* is shown. The derived parameters are presented in *Table 3*.

A more generally useful technique for examining mechanical behaviour of hydrogels is microindentation. We have previously described the use of this technique to study the compression behaviour of hydrogels and in particular its use as an *in vitro* technique to study the response of potential contact lens materials to the eyelid load. The technique is also readily adapted, using a flat-ended indentor, to the determination of crosslink densities of swollen hydrogel materials using a compression modulus technique. It has the advantages that relatively small samples are required, that they may be immersed in a liquid to prevent dehydration and that the temperature of the sample can be controlled between −50 and 90°C. The choice of a spherical indentor of an appropriate size, together with a range of loads, enables equilibrium deformation–recovery values and the derived mechanical properties of the material to be well characterized. The primary form of the results is shown in *Figure 10* which compares indentation–recovery curves (microindentor) with the corresponding load–extension curves (tensometer) for poly(HEMA) and two HEMA–St copolymers. This illustrates the marked change in elastic behaviour accompanying the drop in equilibrium water content, from 38% to 17%, in these three materials. Conversion of indentation–recovery data to compression moduli is important and the most useful relationships in

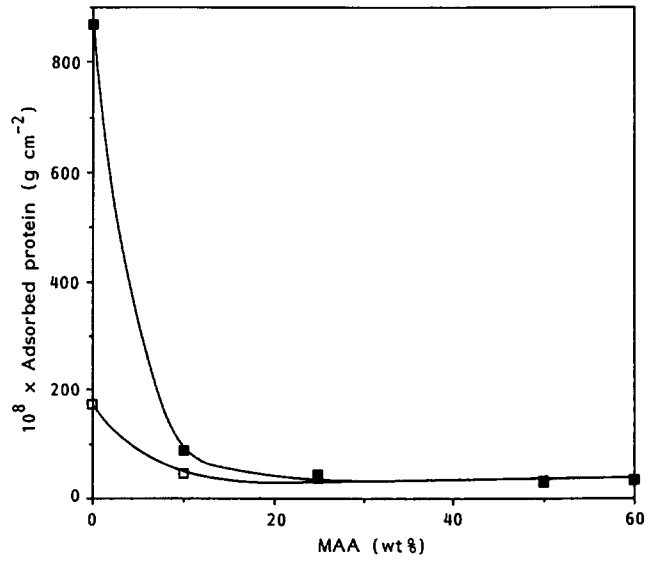

Figure 8 Effect of methacrylic acid incorporation on (■) fibrinogen and (□) albumin absorption of HEMA–MAA copolymer hydrogels

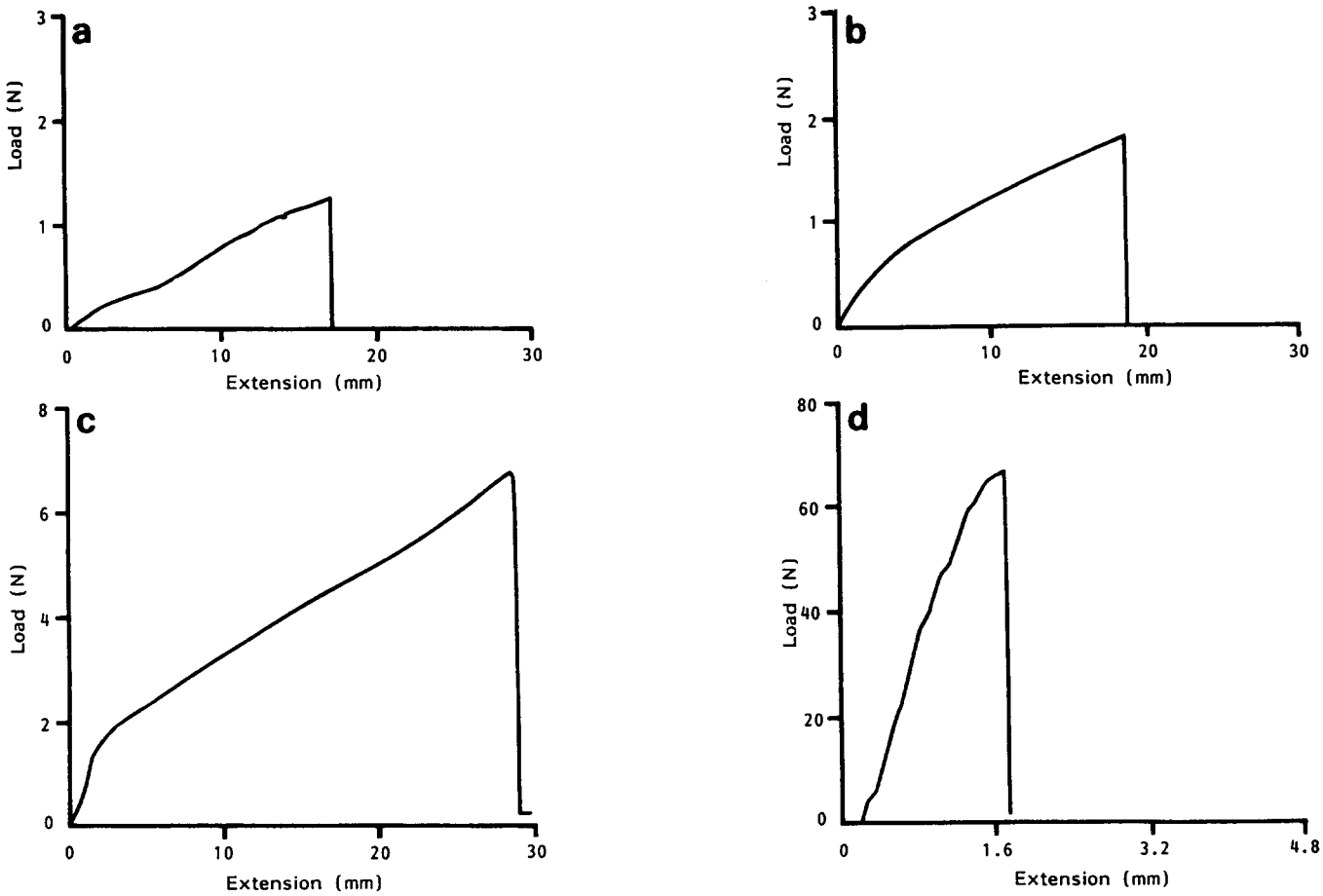

Figure 9 Tensile (load–extension) curves for poly(HEMA) (a) and HEMA–MMA 90/10 (b), 70/30 (c) and 50/50 (d) copolymer hydrogels. Water content data listed in *Table 3*

Table 3 Tensile strength, elongation at break and initial modulus of poly(HEMA) and HEMA–St copolymer hydrogens

Hydrogel composition	*EWC* (%)	Freezing water (%)	Tensile strength (MPa)	Elongation (%)	Initial modulus (MPa)
Poly(HEMA)	37.6	13.2	0.50	198	0.25
HEMA–St 90/10	25.2	2.2	1.32	401	0.37
HEMA–St 80/20	16.7	0.8	7.84	324	2.44
HEMA–MMA 90/10	32.5	7.2	0.35	160	0.22
HEMA–MMA 80/20	27.4	3.4	0.80	241	0.33
HEMA–MMA 70/30	24.1	1.6	0.92	282	0.33
HEMA–MMA 60/40	17.5	0.5	13.17	58	22.71
HEMA–MMA 50/50	12.3	0.0	13.30	21	64.14

this sense are those of Hertz (equation (7)) and Taylor and Kragh (equation (8)). *Figure 11* shows the way in which the primary data may be handled on the basis of the Hertz equation, in order to compare mechanical properties of dehydrated hydroxyalkyl methacrylate polymers, conventional elastomers and hydrogels.

Particular interest centres upon the role of water in relation to changes in mechanical properties. Load–indentation data for hydrated specimens are frequently handled using the equation of Taylor and Kragh which, in general, gives more reproducible results for specimens of this type. *Table 4* summarizes calculated values of rigidity modulus and Young's modulus using both techniques, together with total and freezing water contents, for the materials described here. The way in which water structure affects mechanical properties is additionally illustrated in *Figure 12* in which the mechanical properties of poly(HEMA) determined above and below 0°C are illustrated. There is an apparent similarity between the ability of water to freeze (i.e. the so-called freezing water determined by differential scanning calorimetry) and its ability to plasticize a hydrogel. Further information may be obtained by use of refractometry to investigate the existence of a glass transition temperature in materials of this type. *Figure 13* shows the refractive index of a HEMA–St 95/5 copolymer as a function of temperature. In this figure, two transitions of importance may be observed. The first is the melting point of water within

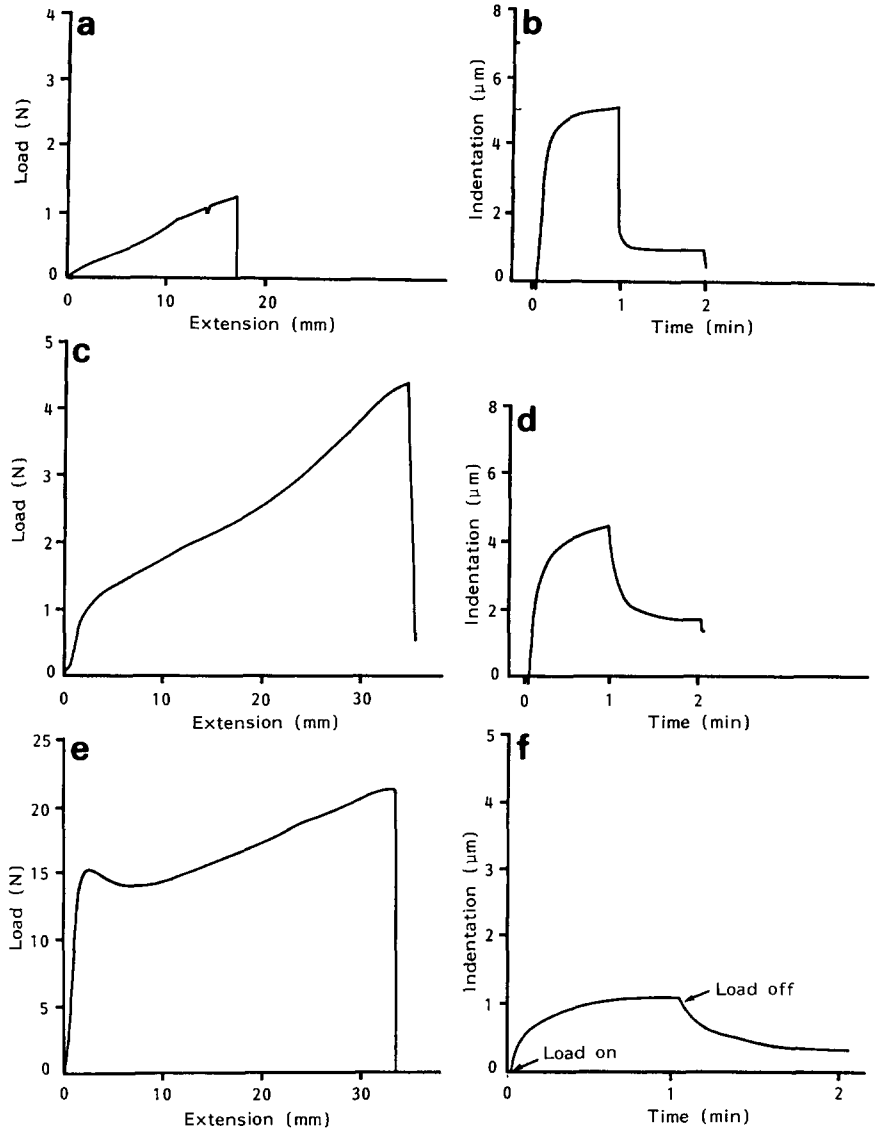

Figure 10 Comparison of tensile (load–extension) and micropenetrometry (load–indentation) profiles for poly(HEMA) (a) and (b), HEMA–St 90/10 (c) and (d) and HEMA–St 80/20 (e) and (f) copolymers

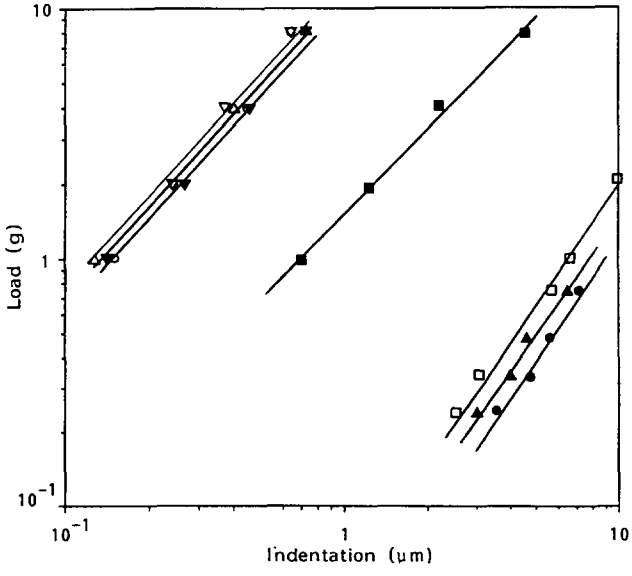

Figure 11 A plot of load *versus* indentation for (▽) poly(MMA), (▼) poly(St), (○) dehydrated poly(HEMA), (△) dehydrated HEMA–St 95/5, (■) dehydrated HEMA–St 80/20, (●) hydrated poly(HEMA), (▲) hydrated HEMA–St 95/5 and (□) EPT

the gel and the steep transition that this produces. The second is the apparent presence of the glass transition (T_g) at around 10°C.

From application of the techniques described here to a range of hydrogels it becomes possible to distinguish between those effects on mechanical properties that derive from the structure of the polymeric material, and those that are controlled by the quantity and state of water binding the material. This may be exemplified by reference to hydrogels based upon the HEMA–St copolymers. On increasing the proportion of styrene in the copolymers two effects can be observed. These may be related to the transition temperatures described above and illustrated in *Figure 13*. One effect is the gradual disappearance of the steep transition occurring at around 0°C. This is associated with increasing styrene content of the copolymer and decreasing freezing water content of the gel. The second effect is the gradual increase of the temperature at which the additional transition, the apparent T_g, occurs. *Figure 14* shows the variation of this transition temperature with the proportion of freezing (i.e. plasticizing) water, as determined by differential scanning calorimetry. It is clear that the structural effects

Table 4 Comparison of values of rigidity modulus and Young's modulus calculated using the Hertz, and Taylor and Kragh equations

Hydrogen composition	*EWC* (%)	Freezing water content (%)	Hertz equation		Taylor and Kragh equation	
			Young's modulus ($N\,m^{-2}$)	Rigidity modulus ($N\,m^{-2}$)	Young's modulus ($N\,m^{-2}$)	Rigidity modulus ($N\,m^{-2}$)
Poly(MMA)	–	–	2.8×10^9	1.1×10^9	5.2×10^8	1.9×10^8
Poly(St)	–	–	2.9	1.1	3.6	1.4
Dehydrated poly(HEMA)	–	–	2.6	1.0	4.9	1.8
Dehydrated HEMA–St 95/5	–	–	2.9	1.1	6.3	2.3
Dehydrated HEMA–St 80/20	–	–	4.3	1.6	5.5	2.1
EPT	–	–	12.0×10^6	4.0×10^6	2.3×10^6	0.9×10^6
Hydrated poly(HEMA)	37.6	13.2	7.1	2.4	1.9	0.5
Hydrated HEMA–St 95/5	29.7	4.8	9.5	3.2	2.6	0.9

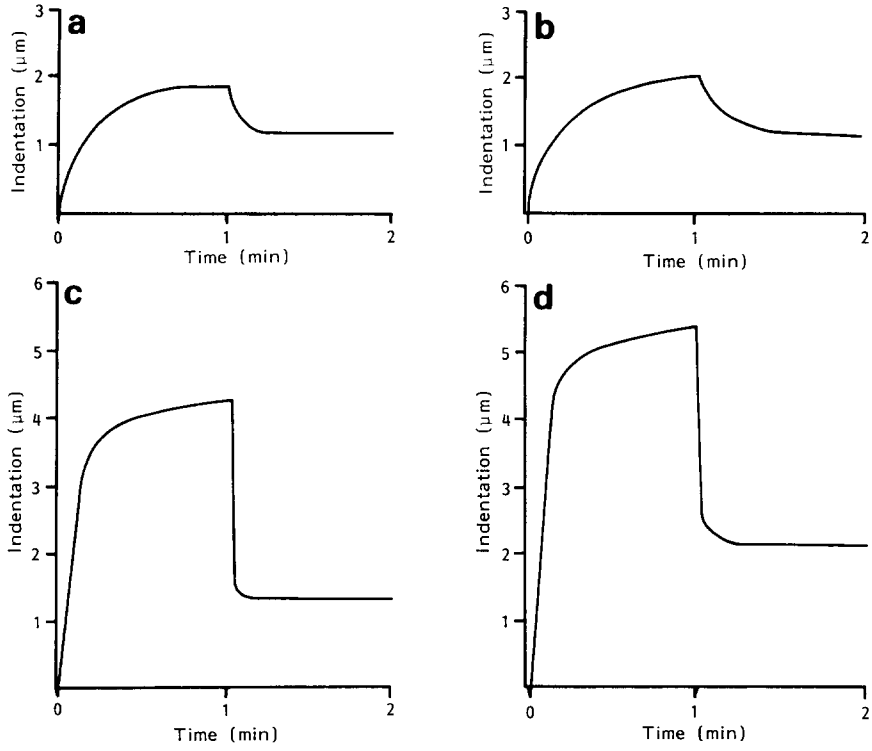

Figure 12 Effect of temperature on the load–indentation profiles for poly(HEMA) hydrogels above and below 0°C: (a) −17°C, (b) −90°C, (c) +12°C and (d) +21°C

observed here are largely independent of changes in transition temperatures associated with modification of the backbone structure in itself (the T_g values of poly(St) and poly(HEMA) and their copolymers are all in the region of 100°C). The effect is then a secondary one, i.e. the effect of monomer structure on the nature and quantity of water in the gel, with this in turn exercising control over the mechanical properties and transport phenomena in the gel.

CONCLUSIONS

It is quite apparent from this study of the surface and mechanical properties of the hydroxyalkyl acrylate and methacrylate copolymers that the dominant effects arise from the control that copolymer composition exerts over *EWC* and water structuring. This is graphically illustrated by the effect of freezing water content on the T_g of the hydrogels (*Figure 14*) which is also reflected in the changes in mechanical properties at room temperature (*Figures 9–12*). Both these phenomena are consequent upon the plasticizing effect of freezing water and contrast with the relatively small effect that non-freezing water seems capable of exerting upon mechanical properties and transition phenomena.

The surface energy changes that are observed within these families are quite dramatic and are illustrated in *Figures 2* and *3*. The increase in fractional polarity

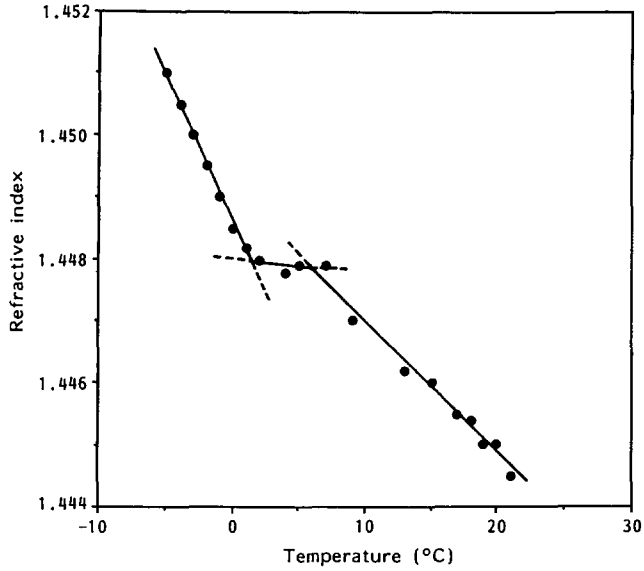

Figure 13 Variation in refractive index with temperature for a hydrated HEMA–St 95/5 copolymer illustrating the water–ice transition and T_g

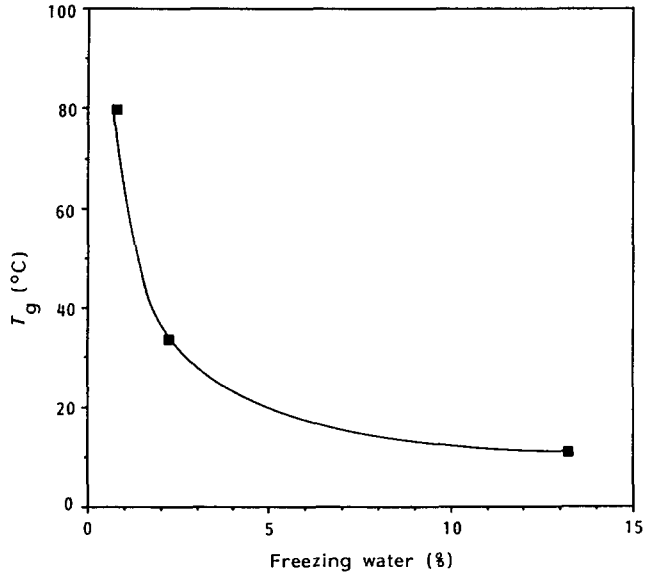

Figure 14 Variation of T_g with freezing water content for HEMA–St copolymer hydrogels

$(\gamma^p/(\gamma^p+\gamma^d))$ on moving from non-hydrated polymers dominated by hydrophobic monomers, such as styrene or methyl methacrylate, to hydrogels of even moderate hydrophilicity, such as those based on poly(HEMA), is most significant. This change in fractional polarity (from around 0.1 or less to 0.6 or greater) corresponds to the difference between commonly encountered, predominantly hydrophobic, synthetic polymers and the level of polarity of natural tissue and biological fluids, dominated as they are by water. It is in the detailed understanding of these phenomena and their relationship with copolymer structure that the greatest potential lies in the design of novel and effective biomaterials.

ACKNOWLEDGMENTS

We are grateful to D. A. Baker, M. S. Chana and D. G. Pedley (co-authors of other parts of this series) for performing parts of this work and to SERC for financial support (A.B.).

REFERENCES

1 Corkhill, P. H., Jolly, A. M., Ng, C. O. and Tighe, B. J. *Polymer* 1987, **28**, 1758
2 Hamilton, W. C. *J. Colloid Interface Sci.* 1972, **40**, 219
3 Owens, D. K. and Wendt, R. C. *J. Appl. Chem. Sci.* 1969, **13**, 1741
4 Macleod, D. B. *Trans. Faraday Soc.* 1923, **19**, 38
5 Fowler, R. H. *Proc. R. Soc. (Lond.) (A)* 1937, **159**, 229
6 Sugden, S. *J. Chem. Soc.* 1924, **125**, 1177
7 Mumford, S. A. and Phillips, J. W. C. *J. Chem. Soc.* 1929, **132**, 2112
8 Hunten, K. W. and Maass, O. *J. Am. Chem. Soc.* 1929, **51**, 153
9 Quayle, O. R. *Chem. Rev.* 1953, **53**, 439
10 Hildebrand, J. H. and Scott, R. L. 'The Solubility of Non Electrolytes', 3rd Edn., Reinhold, New York, 1950
11 Wu, S. *J. Phys. Chem.* 1968, **72**, 3332
12 Small, P. A. *J. Appl. Chem.* 1953, **3**, 71
13 Monk, C. J. H. and Wright, T. A. *J. Oil Colour Chem. Assoc.* 1965, **48**, 520
14 Morris, R. L. J. *J. Oil Colour Chem. Assoc.* 1970, **53**, 761
15 Timoshenko, S. and Goodier, J. N. 'Theory of Elasticity', 2nd Edn., McGraw-Hill, New York, 1951
16 Taylor, D. J. and Kragh, A. M. *J. Phys. (D) Appl. Phys.* 1970, **3**, 29
17 Kaelble, D. *J. Adhes.* 1970, **2**, 66
18 Skelly, P. J. and Tighe, B. J. in preparation
19 Clay, C. S., Lydon, M. J. and Tighe, B. J. in 'Biomaterials and Clinical Applications', (Eds. A. Pizzoferrato, P. G. Marchetti, A. Ravaglioli and A. J. C. Lee), Elsevier Science, Amsterdam, 1987, p. 535
20 Andrade, J. D., King, R. N., Gregonis, D. E. and Coleman, D. L. *J. Polym. Sci., Polym. Symp. Edn.* 1976, **66**, 313
21 Baker, D. A., Corkhill, P. H., Ng, C. O., Skelly, P. J. and Tighe, B. J. *Polymer* 1988, **29**, 691
22 Huang, S. T., Tang, T. E. S. and Kammermeyer, K. J. *J. Macromol. Sci. (B)* 1971,**5**, 1
23 Ng, C. O., Pedley, D. G. and Tighe, B. J. *Br. Polym. J.* 1976, **8**, 124
24 Minett, T. W., Tighe, B. J., Lydon, M. J. and Rees, D. A. *Cell Biol. Int. Rep.* 1984, **8**, 15
25 Lydon, M. J., Minett, T. W. and Tighe, B. J. *Biomaterials* 1985, **6**, 396
26 Bowers, R. W. J. and Tighe, B. J. *Biomaterials* 1987, **8**, 83